International Journal on Recent and Innovation Trends in Computing and Communication
ISSN: 2321-8169 Volume: 10 Issue: 2s
DOI: https://doi.org/10.17762/ijritcc.v10i2s.5954
***Article Received**: 14 October 2022 **Revised**: 18 November 2022 **Accepted**: 26 December 2022*

Two-Dimensionalnumerical Study of the Effect of Nanoparticles on the Fusion and Freezing Process of Phase Change Materials Using a Computing Method

Mohsen Irani*
Faculty of Industry & Mining (Khash), University of Sistan and Baluchestan, Zahedan, Iran
*corresponding author: Mohsen_irani@eng.usb.ac.ir

Abstract
In this paper, a scalar two-dimensional analysis was conducted on the influence of nanoparticles on the thawing and freezing rate of phase-change materials based on enthalpy method that is an innovative calculation method. To this end, carbon nanotubes (CNTs) and aluminum oxide nanoparticles (NPs) were employed as a model of cylindrical and spherical nanoparticles, respectively.Paraffin and a composite of hydrated salts was also utilized as the PCM. The numerical procedure involved the simulation of the phase change process based on finite difference using enthalpy approach. Because of the recent innovations in computer calculation and also its connection with mechanical engineering a computational code was written for this purpose.
Simulation results indicated a reduction in time of thawing and freezing upon incorporation of nanoparticles into the phase change material. For both states, CNTs showed the better result due to acceleration of the heat transfer. The biggest increase (28%) in the rate of thawing and freezing was for CNT-paraffin system; while the lowest increase (6%) was observed in aluminum oxide-hydrated salt system. This result can be utilized to control the speed of energy storage and release.

Keywords: PCM, CNTs, enthalpy method, thawing, freezing.

I. Introduction

The problem of the process rate and its control based on various applications has been of crucial significance in the engineering fields.
The solar wall can be mentioned as an example of the applications requiring various rates of process. Depending on the spaces behind the wall, it may need fast or slow phase change rates for commercial and residential applications. Therefore, the process rate should be controlled depending on system requirements.
In general, the renewable energies should be controlled, stored [1,2], and released. Materials should be adopted to rapidly store these low-cost energies to avoid energy loss. Increasing the thermal conductivity coefficient can be considered as a solution for accelerating the phase change process. Due to high thermal conductivity of nanoparticles, especially CNTs, they could be a proper candidate for this purpose. Numerous studies have addressed the process of freeze-thaw in various materials. In 2011, Sebti et al. [3] numerically assessed heat transfer during the thaw process in two horizontal concentric annular cylinders in the presence of nanoparticles (NPs). A rise was detected in the heat transfer process upon adding NPs. They employed an enthalpy technique through finite volume method to follow the boundaries of solid and liquid phases. Kashani et al. (2014) [4]investigated heat transfer process in an energy storage system with the presence of copper NPs. They reported an increment in the heat release rate upon adding nanoparticles. In 2014, Sherma et al [5] numerically assessed the thawing process of a water-copper oxide nanofluid considering the effect of various contents and temperature difference between the cold and warm parts. They foundthat increasing the amountsof NPs improves heat transfer. In 2018, Irani et al [6] investigated the effect of NPs on the freeze-thaw process of PCMs. Results showed that NPs accelerate the freeze-thaw process. In 2022, Zhang et al. [7] explored the effect of CNTs on paraffin vax as a PCM. They founded that adding CNTs reduces the latent heat by 1.6%.
As mentioned earlier, extensive studies have been conducted onCu_2Oor other NPs. Also, the authors were motivated to examine the influence of CNTs and compared their results with the other NPS. In the present research, the influence of nanoparticle on the freeze-thaw process in phase change was numerically assessed by comparing the performance of different NPs. The purpose of thispaper is tochecking the effect of adding NPsto PCMs on the phase change efficiency.

International Journal on Recent and Innovation Trends in Computing and Communication
ISSN: 2321-8169 Volume: 10 Issue: 2s
DOI: https://doi.org/10.17762/ijritcc.v10i2s.5954
***Article Received**: 14 October 2022 **Revised**: 18 November 2022 **Accepted**: 26 December 2022*

II. Problem definition

2.1. Geometry

The model including the energy storage layer and two adjacent channels are shown in figure 1. The air moves upward in the right channel while it is trapped in the left side. Convection heat transfer occurs on both channels. The dimension of the open channel is $0.005 \times 0.73\ m^2$. The air temperature in the closed left box is 0 and 30℃ during the freezing and melting processes, respectively.In the right channel, air enters at atemperature of 20 ℃ andthis temperature increases based on the free convection heat transfer. Moreover, the constant heat flux of 200 and -200 w/m^2 are intended for the melting and freezing process from the left side of PCM layer, respectively.

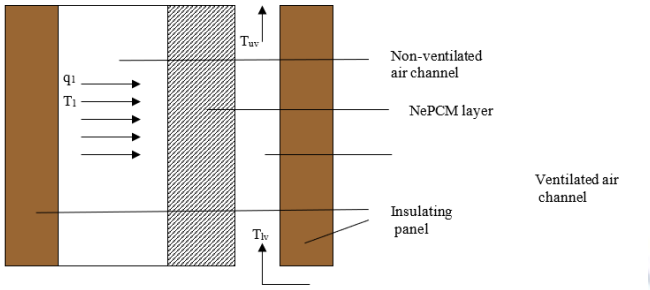

Fig. 1: Geometry of the model

2.2. Materials and basic equations

In this research, air fluid was considered. A combination of hydrated salts [8] and paraffin were also considered as the phase change material. Carbon nanotubes and aluminum oxide NPs were also applied to improve the thermophysical properties as shown in Table 1.

Table 1. variables used in the Thermal Conductivity Equations [6,15]

Parameter	Value	Unit
$d_{np,Al2O3}$, $d_{np,CNT}$, $L_{np,CNT}$	(59,1.7)ⅹ10^{-9}, 5ⅹ10^{-6}	M
$C1_{np,Al2O3}$, $C2_{np,Al2O3}$,c1	0.9830,12.959, -3.91123ⅹ10^{-3}	-
c2, c3, c4	(28.217,3.917,-30.669)ⅹ10^{-3}	-
$s_{1,np,Al2O3}$, $s_{2,np,Al2O3}$	8.4407, -1.07304	-
T_{ref}	298.15	k
K	1.381ⅹ10^{-23}	JK^{-1}
k_1	5ⅹ10^4	-
$C_{p,CNT}$,$C_{p,NP}$	600, 765	J/kg.K
$C_{p,pcm,paraffin}(s,L)$	(1934,2196)	J/kg.K
$C_{p,pcm,hydrated\ salt}(s,L)$	(1832,2207)	J/kg.K
k_{NP}, k_{CNT}	36 , Eq. (15)	W/m.K
$k_{,PCM,paraffin}(s,L)$	(0.358, 0.148)	W/m.K
$k_{,PCM,hydrated\ salt}(s,L)$	(0.82, 0.58)	W/m.K
$\rho_{,PCM,paraffin}(s,L)$	(865,770)	kg/m^3
$\rho_{,PCM,hydrated\ salt}$,ρ_{CNT} , ρ_{NP}	1070 , 1350, 3600	kg/m^3
$L_{pcm,paraffin}$	243	kJ/kg
$T_{m,pcm,paraffin,\ hydrated\ salt}$	27°	C
U	4	$W/m^2.K$

Thermal properties of PCM including latent heat, density, specific heat capacity were predicted. The density of PCMis obtained by:

$$\rho_{\text{eff}} = (1 - \Phi_{\text{vol}})\rho_{\text{PCM}} + \Phi_{\text{vol}}\rho_{\text{NP}} (1)$$

Where, Φ_{vol} denotes the content of the NPs (vol.%). The specific heat capacity of the PCM is obtained by:

(2)

the effective latent heat of the PCM is obtained by:

(3)

The models developed by Zheng et al. [10] and Nan et al. [9] were used to predict the thermal conductivity of PCM based on the non-circular geometry of CNTs.

NANs model for solid phase [9]:

song et al defined a model based on effective length for thermal conductivity [13]. The model developed by Zheng et al. [14] can be regarded as aimproved version of Yamada-Ota's model as follows:

$$\frac{K_{\text{eff}}}{K_b} = \frac{\frac{K_{p,m}}{K_b} + \alpha - \alpha\Phi_N[1-(\frac{K_{p,m}}{K_b})]}{\frac{K_{p,m}}{K_b} + \alpha + \Phi_N[1-(\frac{K_{p,m}}{K_b})]} (5)$$

In comparison with experimental results, the value of 2.1×$5^{-9}\frac{m^2.K}{W}$ is large. This value was taken as the thermal resistance.

The spherical aluminum oxide NPs were also considered. Except for the thermal conductivity, other thermophysical features of the PCM containing Al_2O_3 NPs are similar to the one comprising CNTs. The thermal conductivity of the modified PCMobtained by [15]:

$$k_{n-pcm} = \frac{k_{np} + 2k_{pcm} - 2(k_{pcm} - k_{np})\emptyset_{np}}{k_{np} + 2k_{pcm} + (k_{pcm} - k_{np})\emptyset_{np}} k_{pcm} + \beta k_1 s \rho_{pcm} C_{p,pcm} \sqrt{\frac{KT}{\rho_{np} d_{np}}} f(T, \emptyset_{np}) (6)$$

The first term of this formula is related to the Maxwell model. second sectionrelated to the Brownian motion.

The following equation was employed to calculate the conductivity of CNTs [16]:

$$k = [9.7 \times 10^{-10} T^2 + 3.7 \times 10^{-7} T + 9.3(1 + \frac{0.5}{L_{CNT}}) T^{-2}]^{-1} (7)$$

2.3. Dominant Equations

The following hypotheses were considered:

• The thermal conductivity is the major mechanism involved in the heat transfer.

International Journal on Recent and Innovation Trends in Computing and Communication
ISSN: 2321-8169 Volume: 10 Issue: 2s
DOI: https://doi.org/10.17762/ijritcc.v10i2s.5954
***Article Received**: 14 October 2022 **Revised**: 18 November 2022 **Accepted**: 26 December 2022*

• 2-D heat transfer occurs in x and y directions of the storage wall.
• Thermophysical properties are constant.
• Constant phase change if it happens
• No supercooling and overheating
• change in the volume of the material are ignored

Therefore, the heat transfer in a storage wall equipped with NP-improved phase change materials can be described by [6,17]:

$$\frac{\partial T}{\partial t}=\frac{k_{eff}}{\rho_{eff}C_{p,eff}}\frac{\partial^2 T}{\partial x^2}+\frac{k_{eff}}{\rho_{eff}C_{p,eff}}\frac{\partial^2 T}{\partial y^2}+q_{conv} \qquad)8($$

In the above equation, T, x, y, t, k_{eff} , $C_{p,eff}$ and ρ_{eff} respectively represent temperature, thickness, local dimension perpendicular to thickness, time, thermal conductivity, specific heat capacity [17], and density.

The boundary conditions can be expressed by[17]:

$$\rho_{eff}L\frac{\partial H}{\partial t}=q_1-U[T(0,y,t)-T_1]-k_{eff}\frac{\partial T}{\partial x}\Big|_{x=0}-k_{eff}\frac{\partial T}{\partial y}\Big|_{y}-k_{eff}\frac{\partial T}{\partial y}\Big|_{y+\Delta y} \quad (9)$$

$$\rho_{eff}L\frac{\partial H}{\partial t}=k_{eff}\frac{\partial T}{\partial x}\Big|_{x=L_1}-h_2[T(L_1,t)-T_{mean}]-k_{eff}\frac{\partial T}{\partial y}\Big|_{y}-k_{eff}\frac{\partial T}{\partial y}\Big|_{y+\Delta y} \quad (10)$$

$$\rho_{eff}L\frac{\partial H}{\partial t}=k_{eff}\frac{\partial T}{\partial y}\Big|_{y=0}-k_{eff}\frac{\partial T}{\partial x}\Big|_{x}-k_{eff}\frac{\partial T}{\partial x}\Big|_{x+\Delta x} \quad (11)$$

$$\rho_{eff}L\frac{\partial H}{\partial t}=k_{eff}\frac{\partial T}{\partial y}\Big|_{y=H2}-k_{eff}\frac{\partial T}{\partial x}\Big|_{x}-k_{eff}\frac{\partial T}{\partial x}\Big|_{x+\Delta x} \quad (12)$$

$$\rho_{eff}L\frac{\partial H}{\partial t}=q_1-U[T(0,0,t)-T_1]-k_{eff}\frac{\partial T}{\partial y}\Big|_{y}-k_{eff}\frac{\partial T}{\partial x}\Big|_{x} \quad (13)$$

$$\rho_{eff}L\frac{\partial H}{\partial t}=q_1-U[T(0,H2,t)-T_1]-k_{eff}\frac{\partial T}{\partial y}\Big|_{y}-k_{eff}\frac{\partial T}{\partial x}\Big|_{x} \quad (14)$$

$$\rho_{eff}L\frac{\partial H}{\partial t}=q_1-U[T_{mean}-T(L,0,t)]-k_{eff}\frac{\partial T}{\partial y}\Big|_{y}-k_{eff}\frac{\partial T}{\partial x}\Big|_{x} \quad (15)$$

$$\rho_{eff}L\frac{\partial H}{\partial t}=q_1-U[T_{mean}-T(L,H2,t)]-k_{eff}\frac{\partial T}{\partial y}\Big|_{y}-k_{eff}\frac{\partial T}{\partial x}\Big|_{x} \quad (16)$$

In Eqs. (9)-(16), q_1 ،H ،U ،T_1 ،T_{mean}, and h_2 show absorbed solar flux, enthalpy, total heat transfer coefficient, ambient air temperature, average air temperature within the channel, and heat transfer coefficient.

The phase change materials have variable boundaries as their phase alters from solid to liquid and from liquid to solid. In the enthalpy method, variable boundaries are equated as the mass flow of input or output energies. The transition terms of Eqs. (9)-(16) signify the entrance or exit of the mass-energy flow equivalent to the energy at the beginning and end of the phase change material.

After determining $T(L_1,t)$, the heat flux transferred to the room obtained by:

$$q_{in}=h_2(T(L_1,y,t)-T_{mean}) \quad (17)$$

2.4. Numerical solution

An explicit finite difference numerical approach based on enthalpy method was utilized regarding the nonlinear nature of the governing equations [30,31]. The governing equationswere discretized by the finite difference method:

$$H_{(i,j)}^{p+1}=H_{(i,j)}^{p}+\frac{k_{eff}\Delta t}{\rho_{eff}\Delta x^2}\left(T_{(i+1,j)}^{p}-2T_{(i,j)}^{p}+T_{(i-1,j)}^{p}\right)+\frac{k_{eff}\Delta t}{\rho_{eff}\Delta y^2}\left(T_{(i,j-1)}^{p}-2T_{(i,j)}^{p}+T_{(i,j+1)}^{p}\right) \quad (18)$$

$$H_{(1,j)}^{p+1}=H_{(1,j)}^{p}+\frac{2\Delta t}{\rho_{eff}\Delta x}\Big[q_1+U\left(T_1-T_{(1,j)}^{p}\right)+(k_{eff}/\Delta x)\left(T_{(2,j)}^{p}-T_{(1,j)}^{p}\right)+(k_{eff}\times\Delta x/\Delta y^2)\left(T_{(1,j-1)}^{p}-2T_{(1,j)}^{p}+T_{(1,j+1)}^{p}\right)\Big] \quad (19)$$

$$H_{(M,j)}^{p+1}=H_{(M,j)}^{p}+\frac{2h_2\Delta t}{\rho_{eff}\Delta x}\left(T_{mean}-T_{(M,j)}^{p}\right)+\frac{k_{eff}\Delta t}{\rho_{eff}\Delta y^2}\Big[\left(T_{(M,j-1)}^{p}-2T_{(M,j)}^{p}+T_{(M,j+1)}^{p}\right)+(2\Delta y^2/\Delta x^2)\left(T_{(M-1,j)}^{p}-T_{(M,j)}^{p}\right)\Big] \quad (20)$$

$$H_{(i,1)}^{p+1}=H_{(i,1)}^{p}+\frac{k_{eff}\Delta t}{\rho_{eff}\Delta x^2}\Big[\left(T_{(i+1,1)}^{p}-2T_{(i,1)}^{p}+T_{(i-1,1)}^{p}\right)+(2\Delta x^2/\Delta y^2)\left(T_{(i,2)}^{p}-T_{(i,1)}^{p}\right)\Big] \quad (21)$$

$$H_{(M,j)}^{p+1}=H_{(M,j)}^{p}+\frac{k_{eff}\Delta t}{\rho_{eff}\Delta x^2}\Big[\left(T_{(i+1,N)}^{p}-2T_{(i,N)}^{p}+T_{(i-1,N)}^{p}\right)+(2\Delta x^2/\Delta y^2)\left(T_{(i,N-1)}^{p}-T_{(i,N)}^{p}\right)\Big] \quad (22)$$

$$H_{(1,1)}^{p+1}=H_{(1,1)}^{p}+\frac{2\Delta t}{\rho_{eff}\Delta x}q_1+\frac{2k_{eff}\Delta t}{\rho_{eff}\Delta x^2}\Big[\left(T_{(2,1)}^{p}-T_{(1,1)}^{p}\right)+(\Delta x^2/\Delta y^2)\left(T_{(1,2)}^{p}-T_{(1,1)}^{p}\right)\Big] \quad (23)$$

$$H_{(1,N)}^{p+1}=H_{(1,N)}^{p}+\frac{2\Delta t}{\rho_{eff}\Delta x}q_1+\frac{2k_{eff}\Delta t}{\rho_{eff}\Delta x^2}\Big[\left(T_{(2,N)}^{p}-T_{(1,N)}^{p}\right)+(\Delta x^2/\Delta y^2)\left(T_{(1,N-1)}^{p}-T_{(1,N)}^{p}\right)\Big] \quad (24)$$

$$H_{(M,1)}^{p+1}=H_{(M,1)}^{p}+\frac{2h_2\Delta t}{\rho_{eff}\Delta x}\left(T_{mean}-T_{(M,1)}^{p}\right)+\frac{2k_{eff}\Delta t}{\rho_{eff}\Delta x^2}\Big[\left(T_{(M-1,1)}^{p}-T_{(M,1)}^{p}\right)+(\Delta x^2/\Delta y^2)\left(T_{(M,2)}^{p}-T_{(M,1)}^{p}\right)\Big] \quad (25)$$

$$H_{(M,N)}^{p+1}=H_{(M,N)}^{p}+\frac{2h_2\Delta t}{\rho_{eff}\Delta x}\left(T_{mean}-T_{(M,N)}^{p}\right)+\frac{2k_{eff}\Delta t}{\rho_{eff}\Delta x^2}\Big[\left(T_{(M-1,N)}^{p}-T_{(M,N)}^{p}\right)+(\Delta x^2/\Delta y^2)\left(T_{(M,N-1)}^{p}-T_{(M,N)}^{p}\right)\Big] \quad (26)$$

International Journal on Recent and Innovation Trends in Computing and Communication
ISSN: 2321-8169 Volume: 10 Issue: 2s
DOI: https://doi.org/10.17762/ijritcc.v10i2s.5954
***Article Received**: 14 October 2022 **Revised**: 18 November 2022 **Accepted**: 26 December 2022*

Using the enthalpy method, the governing equation (Eq. (1)) and boundary conditions were transformed into Eqs. (17)-(25) where, the enthalpy term is obtained based on the temperature of the PCM in terms of tangible and latent heats (phase change).[30] A computational code was developed based on Eqs. (17) to (25) for prediction of the thermal behavior of the PCM layer.

The temporal and spatial steps of the numerical solution were determined according to network independence. Since the explicit method is utilized for numerical solution of the problem, the temporal and spatial steps should apply to the Courant stability criterion in the following two-dimensional formalation [30].

$$\frac{\rho C_{p,PCM}}{2} \geq \frac{k_{PCM}dt}{dx^2} + \frac{k_{PCM}dt}{dy^2} \quad (27)$$

Where, Δt represents the temporal step while $\Delta x = L_1/N$ and $\Delta y = H_1/M$ denote the spatial steps of the numerical solution network. Based on Fig. 2, the storage wall can be divided into N × M nodes.

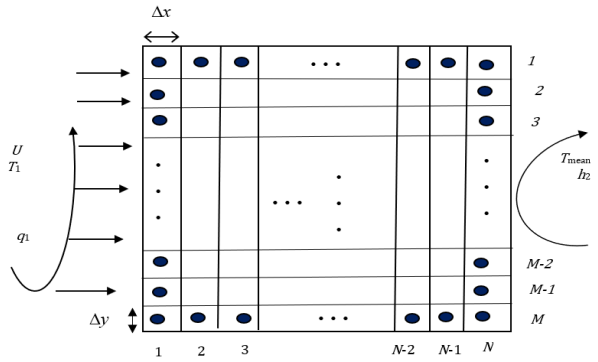

Figure.2 Discrete grid of a solar wall used in the two-dimensional numerical solution

let that air enter the airflow channel at room temperature (RT). Assuming one-dimensional heat transfer of the airflow along the the length of the channel, the temperature of the output hot air entering the chamber can be obtained by [32]:

$$T_{UV} = (T_{LV} - T_N^p)exp^{-\frac{h_2 b}{\dot{m}C_{p,air}}H_2} + T_N^p \quad (28)$$

$$T_{mean} = (T_{LV} + T_{UV})/2 \quad (29)$$

$$\dot{m} = \rho_{air}A_s\sqrt{\frac{0.5g\beta_{air}(T_{UV} - T_{LV})H_2 + \Delta P/\rho_{air}}{0.41Gr^{0.084}H_2/D_h + 2.5(A_s/A_v)^2}} \quad (30)$$

Where, T_{UV}, T_{LV} stand for air temperature at the channel outlet and inlet , respectively. Moreover, T_{mean} shows bulk temperature in the right channel. h_2 ،b ،$\dot{m}$ ،C_p, and H_2, also represent heat transfer coefficient of airflow, channel width, mass flow rate within the channel, the air specific heat capacity, and height of the channel, respectively. The free convection coefficient h_2 can be numerically determined based on the mean Nusselt relation [13]. Here, the Rayleigh number (Ra_H)can be determined based on T_N^p and T_{mean}.

$$\overline{Nu}_H = 0.68 + \frac{0.67Ra_H^{0.25}}{[1 + (0.492/Pr)^{9/16}]^{4/9}} \quad (31)$$

III. Results and discussions:

A two-dimensional scalar simulation was studied in this paper to assess the effect of NPs on the freeze-thaw process of PCMs. To this end, a computational code was developed in MATLAB software based on the mentioned equations, to evaluated the influence of the nanoparticles on the PCMs, once the pure PCM and then the CNT-PCM and Al_2O_3-PCM systems were assessed. The content of the CNTs was 5 vol.%. fig. 3 presented the freezing of various material at the same moment, as seen, the temperature reduction was higher in the case with CNTs; while the lowest temperature decrement was for the pure PCM.

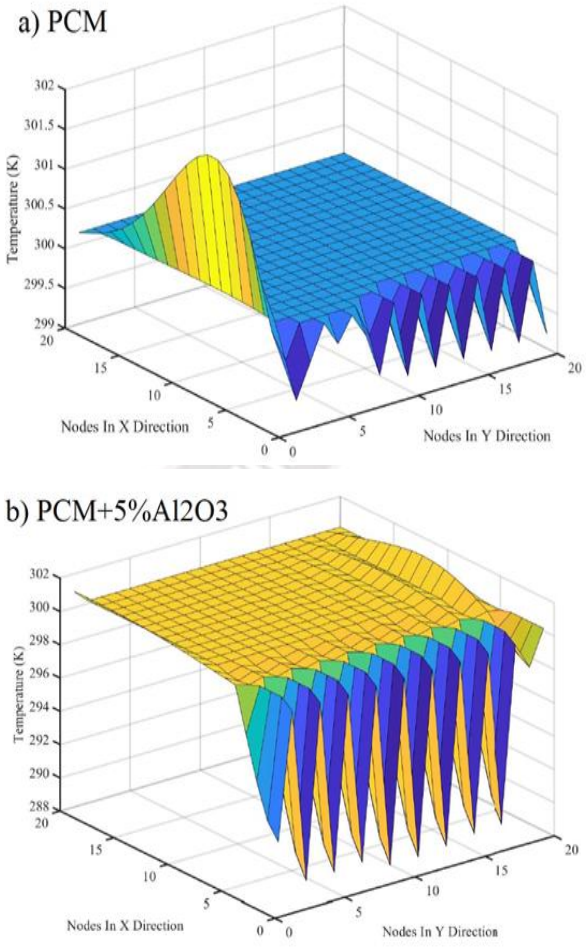

International Journal on Recent and Innovation Trends in Computing and Communication
ISSN: 2321-8169 Volume: 10 Issue: 2s
DOI: https://doi.org/10.17762/ijritcc.v10i2s.5954
***Article Received**: 14 October 2022 **Revised**: 18 November 2022 **Accepted**: 26 December 2022*

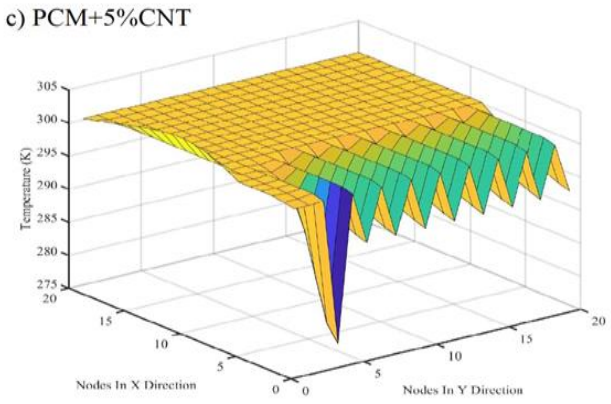

Fig. 3: A view of paraffin layer with various nodes a) PCM, b)PCM+Al_2O_3, c)PCM+CNT

The rate of the freeze-thaw process was evaluated in the NP-enhanced PCMs containing 5 vol% CNT or Al_2O_3 NPs. Higher NP contents were not considered as the stability of the system may be disturbed at higher contents of nanoparticles. The durations of the thawing and freezing processes of paraffin containing various NPs contents were determined as presented in Figs. 4 and 5.

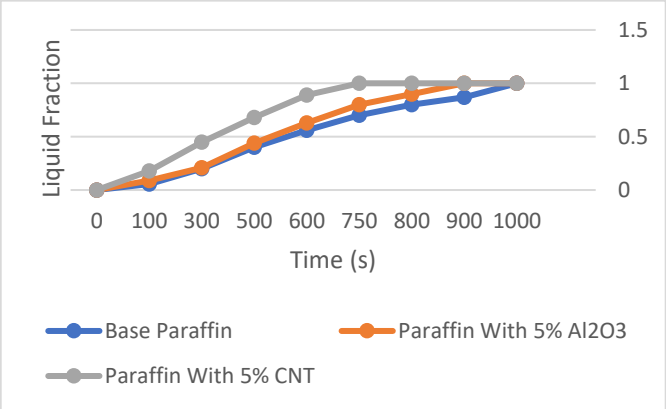

Fig. 4: Thawing rate of pure and NP-enhanced paraffin

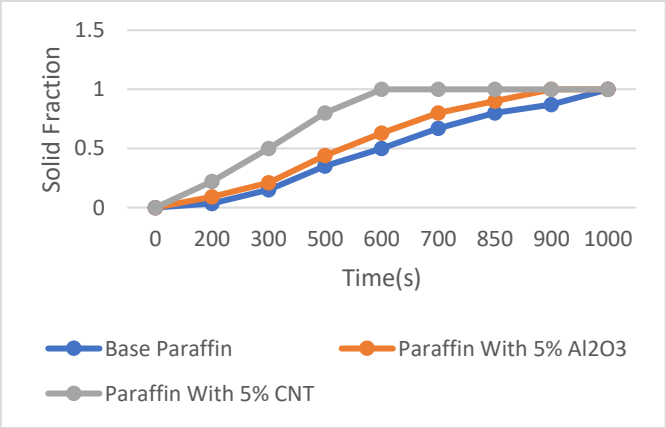

Fig. 5: Freezing rate of pure and NP-enhanced paraffin

According to Figs. 4 and 5, the incorporation of CNTs and Al_2O_3 NPs enhanced the thaw and freezing process in the paraffin. Meanwhile, CNT caused a higher enhancement which can be assigned to its far higher thermal conductivity compared to Al_2O_3 NPs. The thawing rate of paraffin was enhanced by 30 and 16% upon adding CNTs and Al_2O_3 NPs, respectively. For the freezing process the increment in the rate of freezing was 14.5 and 5.5%, respectively. Figs 6 and 7 also illustrate the thawing and freezing durations for the other PCM (a combination of hydrated salts). Based on these two figures, similar to the case of paraffin, the rate of the thawing-freezing processes was enhanced upon adding the mentioned NPs.

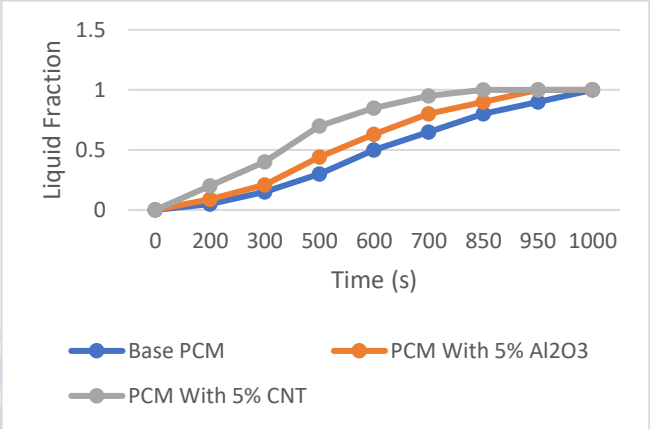

Fig. 6: Thawing process of NP-modified hydrated salts

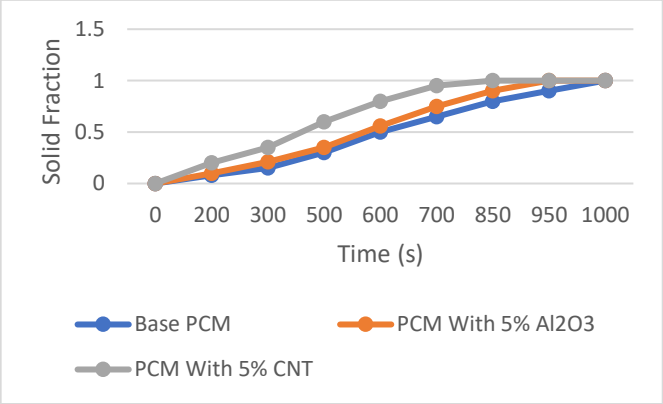

Fig. 7: Freezing process of NP-modified hydrated salts

In this research, the process time curves were plotted by assigning the longest duration to 100 and normalizing the other results based on that.

International Journal on Recent and Innovation Trends in Computing and Communication
ISSN: 2321-8169 Volume: 10 Issue: 2s
DOI: https://doi.org/10.17762/ijritcc.v10i2s.5954
***Article Received**: 14 October 2022 **Revised**: 18 November 2022 **Accepted**: 26 December 2022*

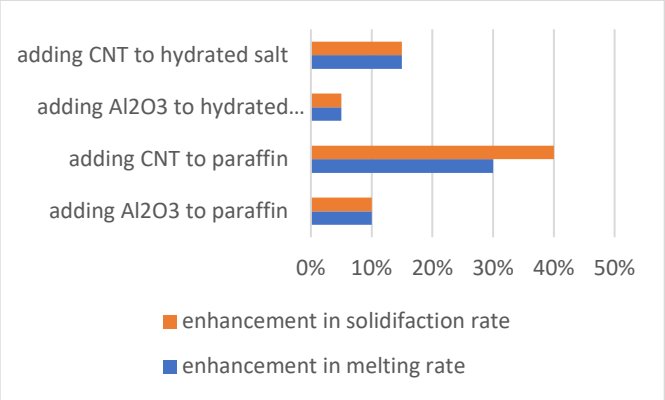

Fig. 8: The effect of NPs on the thaw-freeze rate of PCMs compared to the pure states.

According to Fig. 8, the highest increment in the process rate was for the case where CNT was added to paraffin. This behavior can be assigned to two major reasons:
1- low conductivity of paraffin
2-ultrahigh conductivity of CNT.
Moreover, lowest rise in the process rate compared to the pure cases was for the system comprising Al2O3 NPs and hydrated salts. For better understanding of the reasons behind the acceleration of the heat transfer, Table 3 lists the thermal conductivity of different materials.
according to Table 2 and the results of the thaw-freeze rate of various materials, the enhancement of the thermal conductivity directly affects the thaw-freeze rate.

Table 3: Thermal conductivity of various materials

Material	K (W/mK)
Paraffin	0.148
Paraffin+CNT 5%	4.8
Paraffin+ Al_2O_3 NPs 5%	0.85
Hydrated salts	0.58
Hydrated salts+CNT 5%	5.1
Hydrated salt+ Al_2O_3 NPs 5%	0.93

IV. Conclusions

In this article, a numerical study carried out to determine the speed of fusion and freezing process of pure PCM and improved PCM.
Based on the simulation results a decrease on the duration of the thawing and freezing processes upon the incorporation of NPs to PCMs was shown. For both PCMs, CNTs exhibited better performance in accelerating the heat transfer as compared to Al_2O_3. The highest (28%) and lowest (6%) acceleration in the freeze-thaw processes compared to the pure condition was for paraffin+CNT and hydrated salt+Al_2O_3. Therefore, thermal performance of the PCMs was improved with the presence of Al_2O_3 and CNTs. For both improved states, the thermal performance of the modified PCM was better than the base state; however, the incorporation of CNTs led to better outcomes compared to Al_2O_3. generally the use of NPs accelerated the freeze-thaw process. However using of NPs has no economicjustification for energystorage operations which can be achieved at low costs using the conventional methods.

List of Symbols

C_p: Specific heat capacity, $\frac{j}{kg.k}$
K: Thermal conductivity coefficient, $\frac{w}{m.k}$
H: enthalpy or total energy content , $\frac{j}{kg}$
H: heat transfer coefficient, $\frac{W}{m^2.k}$
Q_1: input flux, $\frac{W}{m^2}$
T: temperature, ℃

Greek signs

P: density, kg / m3

Subtitle

Nepcm: nanoparticle-enhancedPCM
PCM: phase-change material
I: node number
Np: nano particle
1: Parameters related to the left closed channel
2: Parameters related to the open right channel

Superscript

P: Time step

References

[1]. Mashhour A.Alazwari, MohammedAlgarni, Mohammad RezaSafaei,"Effects of various types of nanomaterials on PCM melting process in a thermal energy storage system for solar cooling application using CFD and MCMC methods,"International Journal of Heat and Mass Transfer.Volume 195, October 2022, 123204.
[2]. Ao. Li, Shuangping. Duan, Rubing. Han, Chaoyu. Wang, "Investigation on the dynamic thermal storage/release of the integrated PCM solar wall embedded with an evaporator,"Renewable Energy, Available online 4 October 2022
[3]. S.S.Sebti, SH.Khalilarya, I.Mirzaee, S.F. Hosseinizadeh, S.Kashani ,M.Abdollahzadeh",A Numerical Investigation of solidification in Horizontal Concentric Annuli Filled with Nano-Enhanced Phase change Material (NEPCM)," World Applied Sciences Journal 13 (1), 09-15, 2011
[4]. S. Kashani, E.Lakzian, K.Lakzian, M.Mastiani",Numerical Analysis Of Melting Of Nanoenhanced Phase Change Material In Laten Heat Thermal Energy Storage System," THERMAL SCIENCE, Vol. 18, S335-S345. 2014.

International Journal on Recent and Innovation Trends in Computing and Communication
ISSN: 2321-8169 Volume: 10 Issue: 2s
DOI: https://doi.org/10.17762/ijritcc.v10i2s.5954
***Article Received**: 14 October 2022 **Revised**: 18 November 2022 **Accepted**: 26 December 2022*

[5]. R.K.Sharma, P.Ganesan",Solidification Of Nano-Enhanced Phase Change Materials (NEPCM) In a Trapezoidal Cavity: A CFD study," Universal Journal of Mechanical Engineering2(6), 187-192, 2014.

[6]. Mohsen Irani, Faramarz Sarhaddi, Amin Behzadmehr, "Numerical investigation of the effect of nanoparticles on thermal efficiency of phase change materials," Acta Technica 63 No. 4/2018, 625–632

[7]. Yuanying Zhang, Daili Feng, Yanhui Feng, Xinxin Zhang, "Effect of carbon nanotubes on melting latent heat of paraffin wax: An experimental and simulated research,"Journal of Energy Storage,Volume 53, September 2022, 105229

[8]. Zohir Younsi1, Laurent Zalewski1, Daniel R. Rousse, "THERMOPHYSICAL CHARACTERIZATION OF PHASE CHANGEMATERIALS WITH HEAT FLUX SENSORS," 5th European Thermal- Sciences Conference, The Netherlands, 2008.

[9]. Nan, C. W, Liu. G, Lin. Y, and Li. M, "Interface Effect on Thermal Conductivity of Carbon Nanotube Composites," Applied Physics Letters, Vol. 85, No. 16, pp. 3549–3551, 2004.

[10]. Pop, E., Mann, D., Cao, J., Wang, Q., Goodson, K., Dai, H. "Thermal Conductance of an Individual SingleWall Carbon Nanotube above Room Temprature," Nano Letters 6, pp. 96-100, 2006.

[11]. R.K.Sharma, P.Ganesan , "Solidification Of Nano-Enhanced Phase Change Materials (NEPCM) In a Trapezoidal Cavity: A CFD study," Universal Journal of Mechanical Engineering2(6), 187-192, 2014.

[12]. S. Kashani, E.Lakzian, K.Lakzian, M.Mastiani, "Numerical Analysis Of Melting Of Nanoenhanced Phase Change Material In Laten Heat Thermal Energy Storage System," THERMAL SCIENCE, Vol. 18, S335-S345. 2014.

[13]. Song, P., Liu, C., and Fan, S., "Improving the Thermal Conductivity of Nanocomposites by Increasing the Length Efficiency of Loading Carbon Nanotubes," Applied Physics Letters, Vol. 88, pp. 153111, 2006.

[14]. Ying song Zhengand Haiping Hong, "Modified Model for Effective Thermal Conductivity of Nanofluids ContainingCarbon Nanotubes," JOURNAL OF THERMOPHYSICS AND HEAT TRANSFER. Vol. 21, No. 3, pp. 658-660, 2007.

[15]. A. ValanArasu , Agus P. Sasmito, Arun S. Mujumdar,"THERMAL PERFORMANCE ENHANCEMENT OF PARAFFIN WAX WITHAL2O3 CuO NANOPARTICLES A NUMERICAL STUDY," Frontiers in Heat and Mass Transfer (FHMT), 2, 043005 , 2011.

[16]. Hone,J., "Carbon Nanotubes: Thermal Properties" Dekker Encyclopedia of Nanoscience and Nanotechnology,pp.603-610, 2004.

[17]. K. peippo, P. Kauranen, P.D.Lund, "A multicomponent PCM wall optimized for passive solar heating," Energy and Building 17, Pp. 259-270, 1991.